Supplementary Information

Designing electrolyte structure to suppress hydrogen evolution reaction in aqueous batteries

Qingshun Nian et al.

Supplementary Figures

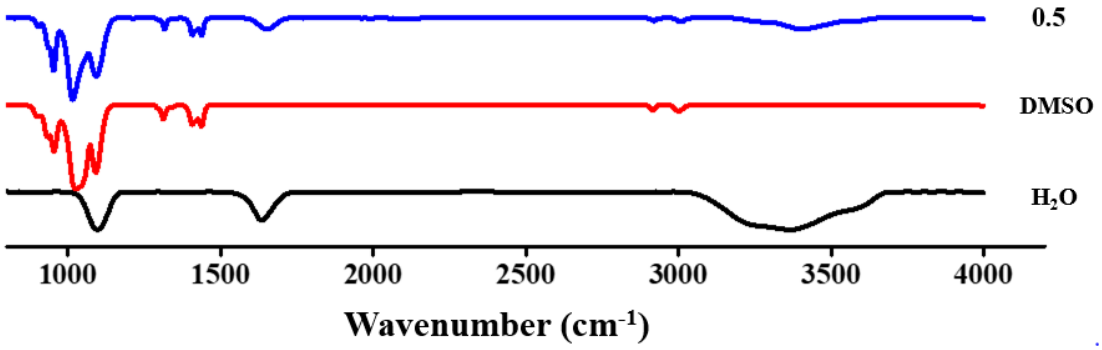

Supplementary Fig. 1 Component analysis of DMSO and water mixed solution. FTIR spectra of pure water, pure DMSO and DMSO/water mixed solution.

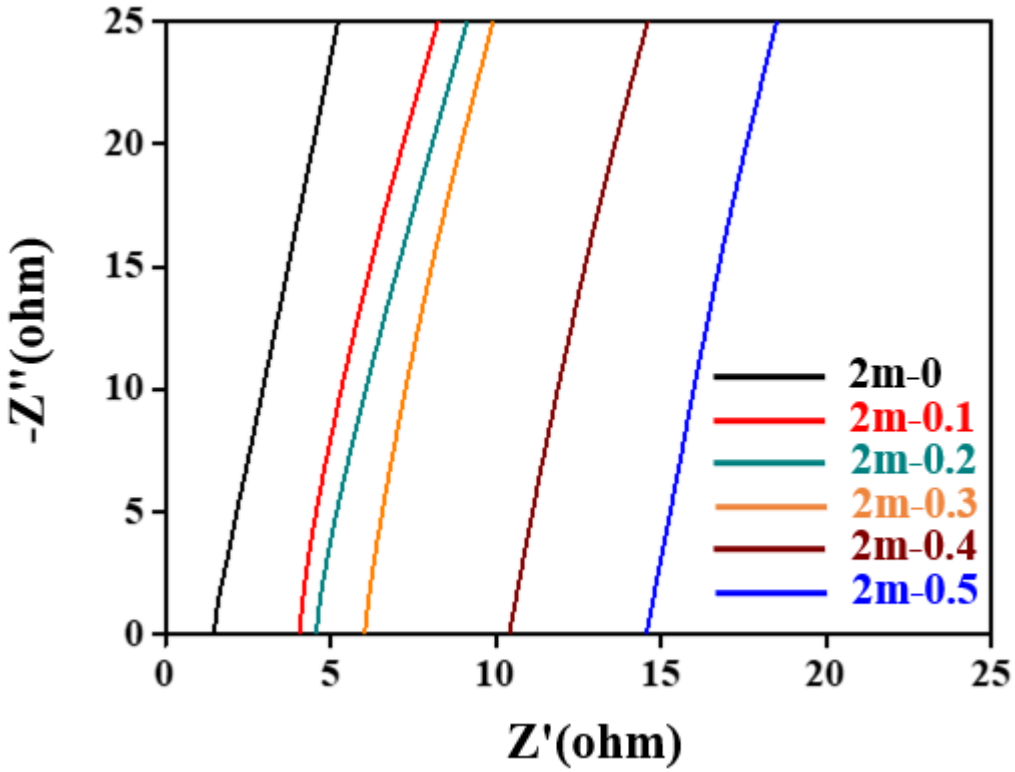

Supplementary Fig. 2 Electrolyte impedance analysis. Electrochemical impedance spectroscopy (EIS) of 2 m $NaClO_4$ with different mole fractions of DMSO.

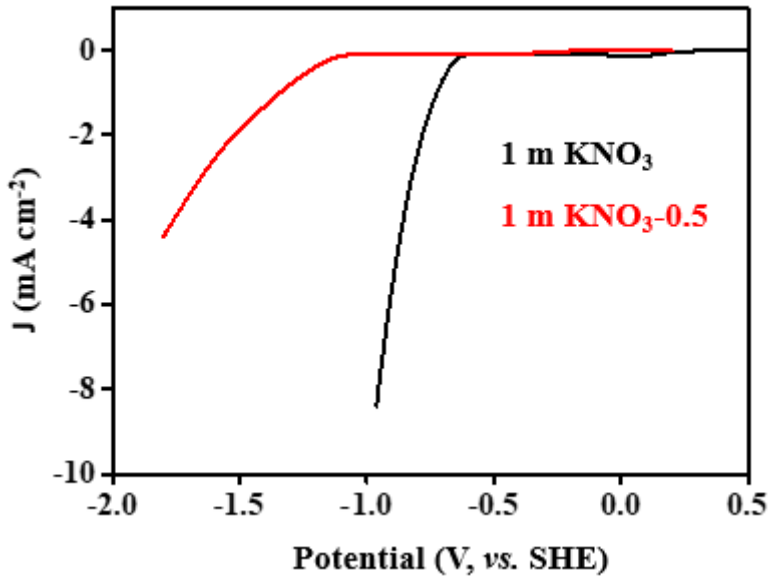

Supplementary Fig. 3 Hydrogen evolution window. Linear voltammetry curves recorded at 10 mVs^{-1} in 1 m KNO_3 and 1 m KNO_3-0.5 aqueous electrolytes.

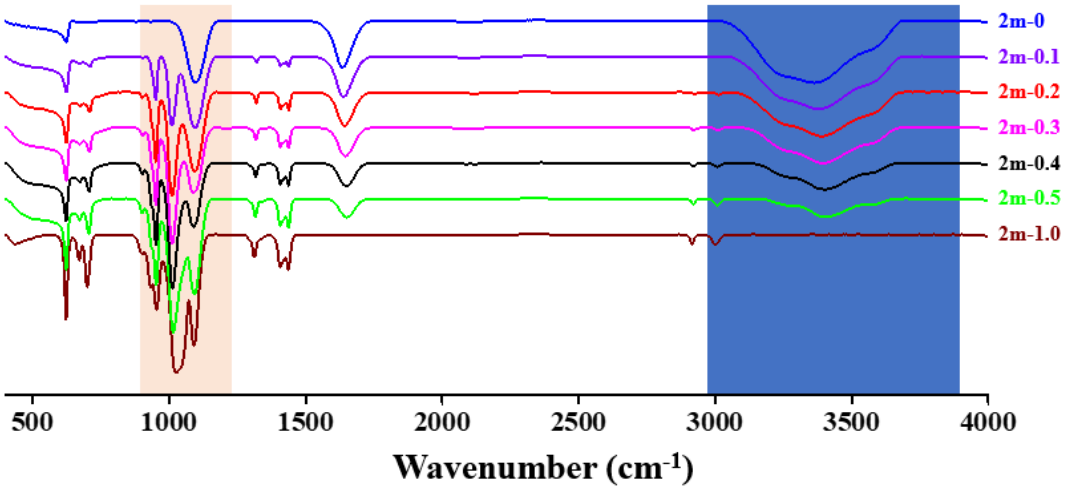

Supplementary Fig. 4 FTIR spectra of electrolyte. FTIR spectra of 2 m $NaClO_4$ with different mole fractions of DMSO (0, 0.1, 0.2, 0.3, 0.4, 0.5, 1.0), from which can be detected that the signal at maroon area is the S=O vibration band, and blue area is the O-H stretching band of water.

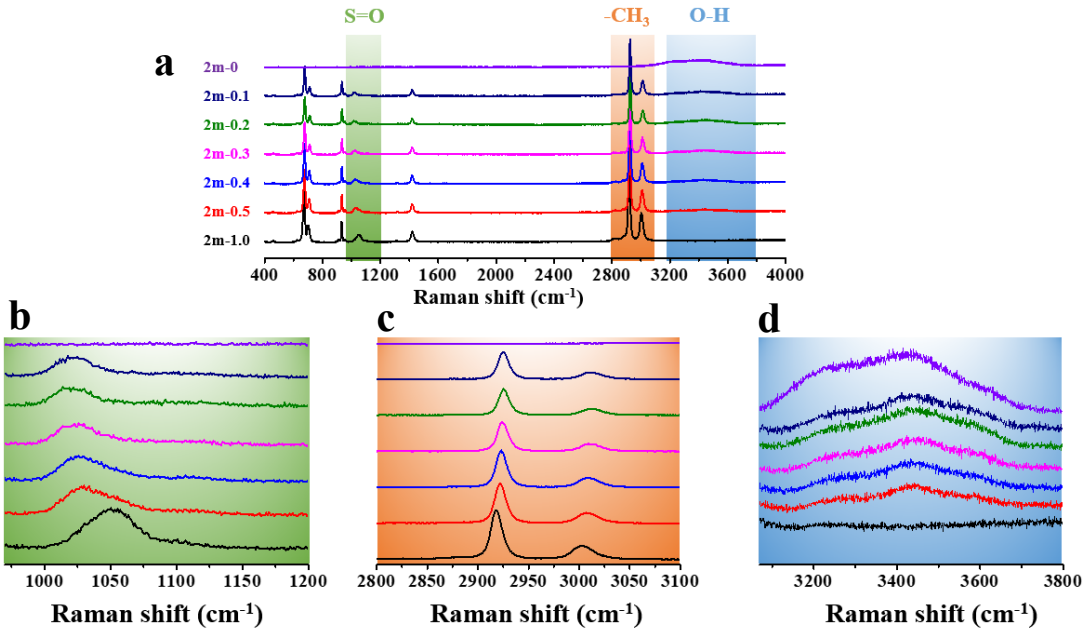

Supplementary Fig. 5 Raman spectra of electrolyte. a Raman spectra of 2 m $NaClO_4$ with different mole fractions of DMSO (0, 0.1, 0.2, 0.3, 0.4, 0.5, 1.0). **b**, **c**, **d** Partial enlargement view of Fig. **a**.

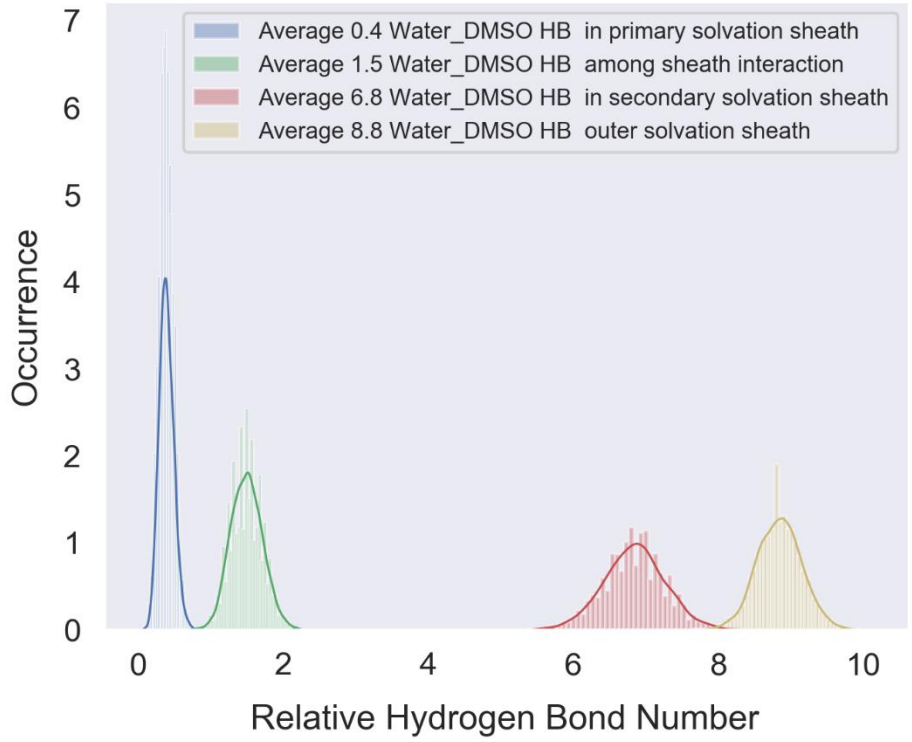

Supplementary Fig. 6 Relative hydrogen bond number distribution within Na^+ hydration sheath in 2 m-0.5 $NaClO_4$-DMSO system.

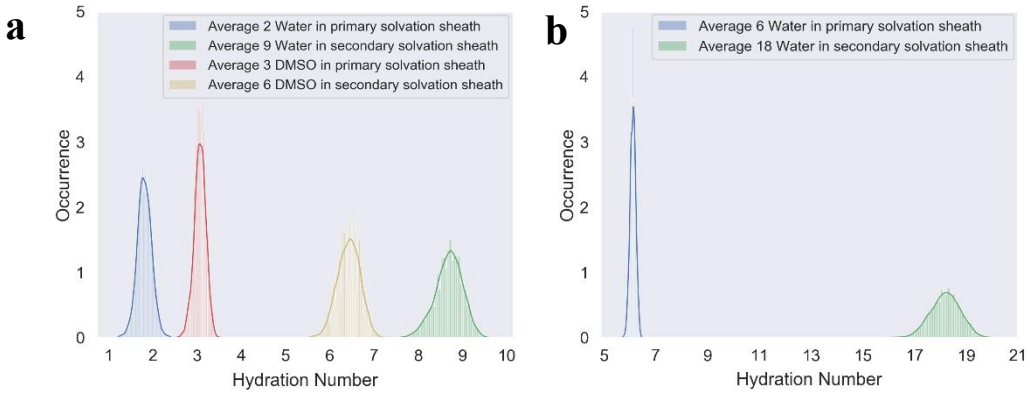

Supplementary Fig. 7 Hydration number distribution in different sheath for systems of a) 2 m-0.5 $NaClO_4$-DMSO and b) 2 m $NaClO_4$

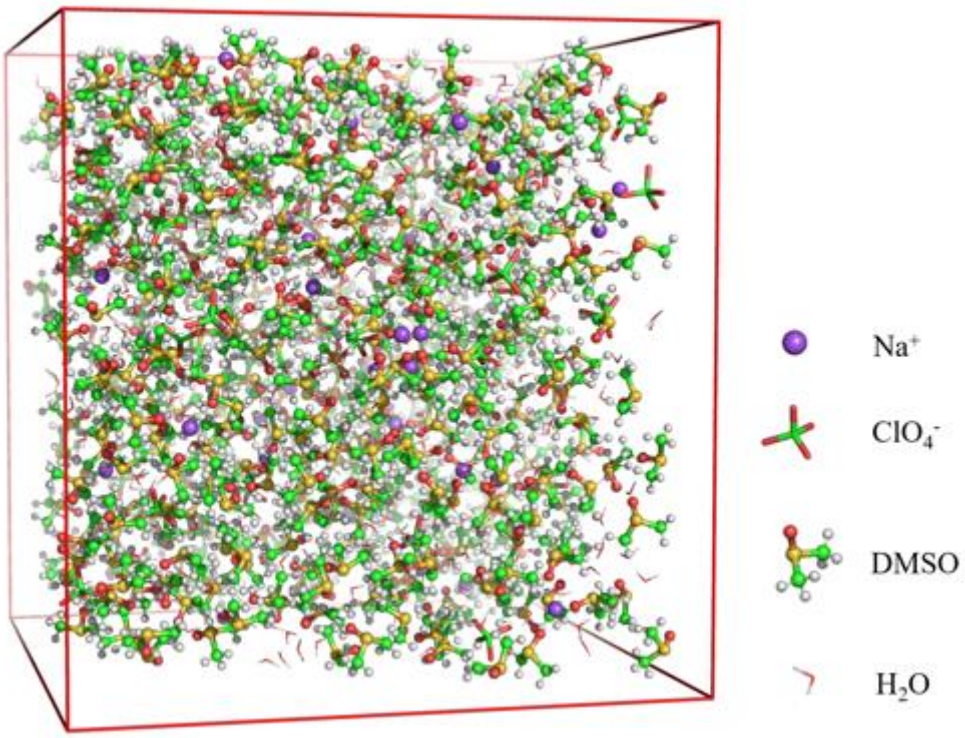

Supplementary Fig. 8 MD simulations of the Na^+-solvation structure. Snapshots of MD simulation boxes for systems of 2 m-0.5 $NaClO_4$-DMSO at 100 ns timestamp.

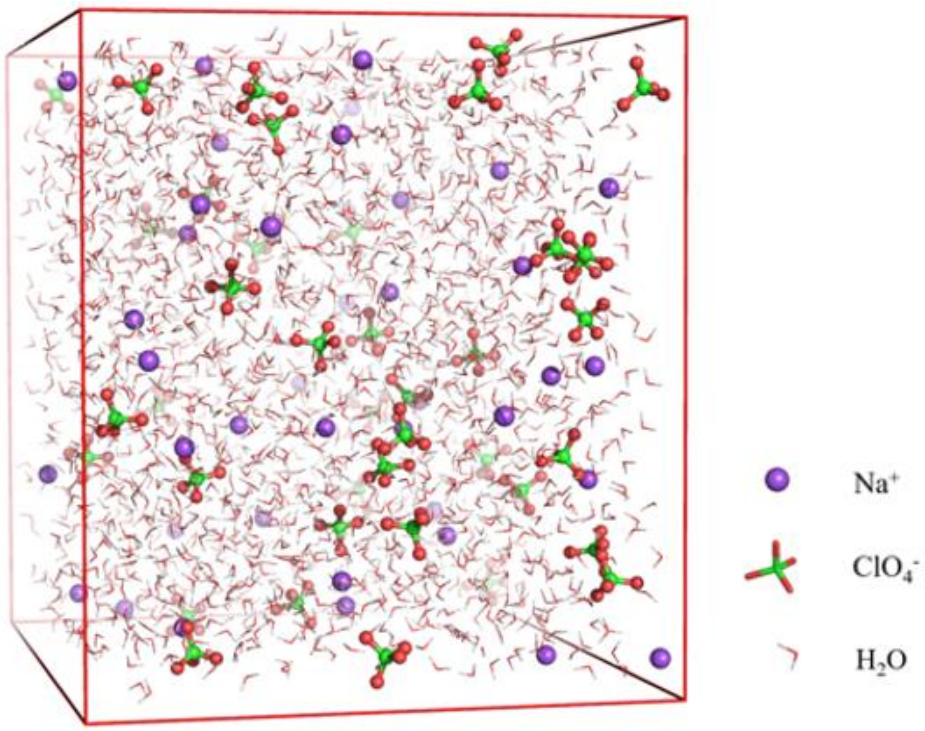

Supplementary Fig. 9 MD simulations of the Na^+-solvation structure. Snapshots of MD simulation boxes for systems of 2 m $NaClO_4$ at 100ns timestamp.

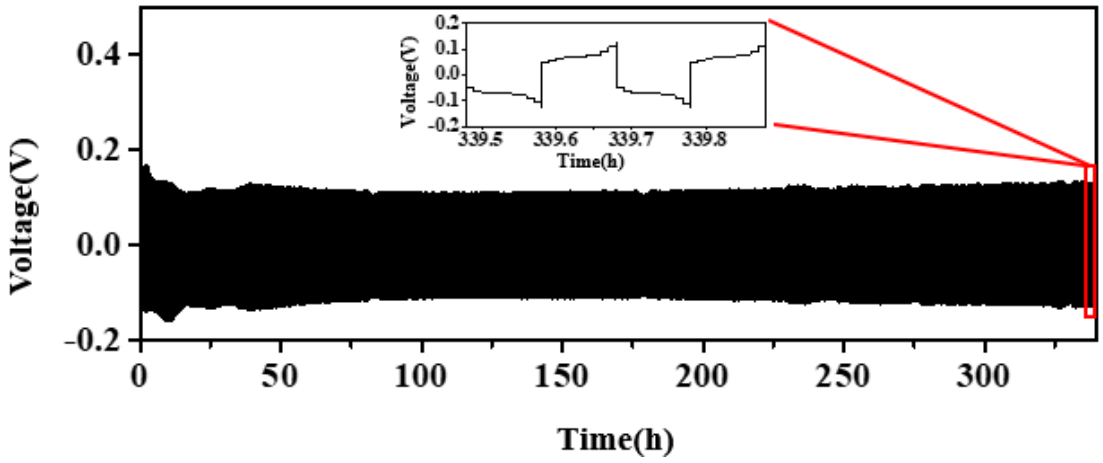

Supplementary Fig.10 Galvanostatic cycling performance of symmetric Zn/Zn cells tests using 2 m $Zn(CF_3SO_3)_2$-0.5 electrolyte. High rate of 5 mA cm^{-2} (0.5 mAh cm^{-2} for each half cycle).

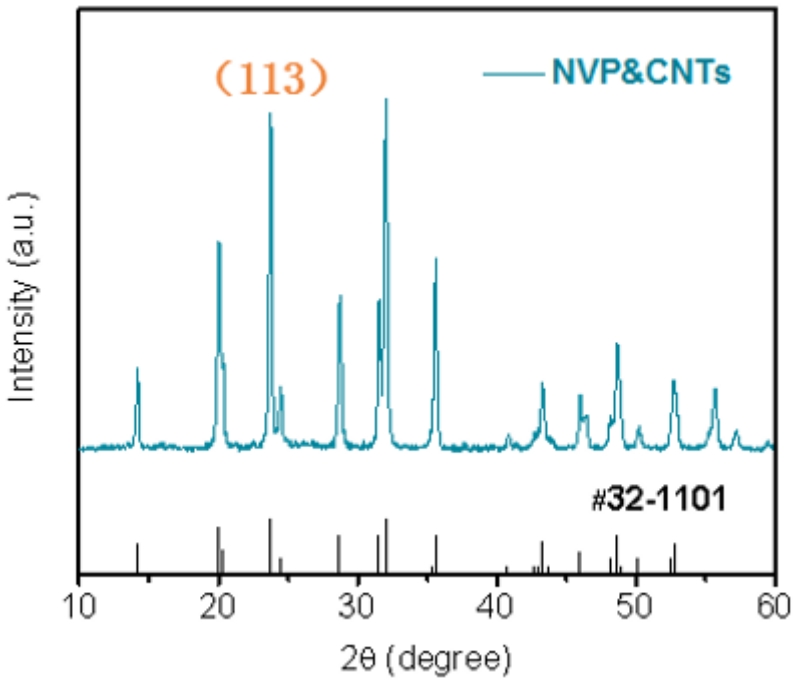

Supplementary Fig. 11 Characterization of as-prepared $Na_3V_2(PO_4)_3$&CNTs (NVP&CNTs) powder. XRD pattern. It can be detected from the XRD pattern that all the diffraction peaks are accurately indexed to the NASICON structured NVP with R-$\bar{3}$c space group (JCPDS No. 32-1101), which demonstrated the successful preparation of NVP&CNTs.

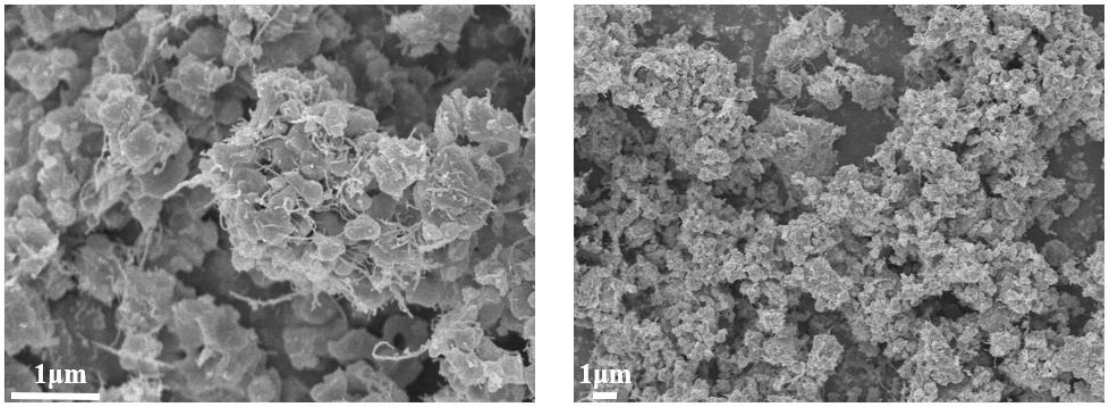

Supplementary Fig. 12 Morphology analysis of the electrode materials.

SEM of NVP&CNTs indicate that the NVP cross-linked with CNTs.

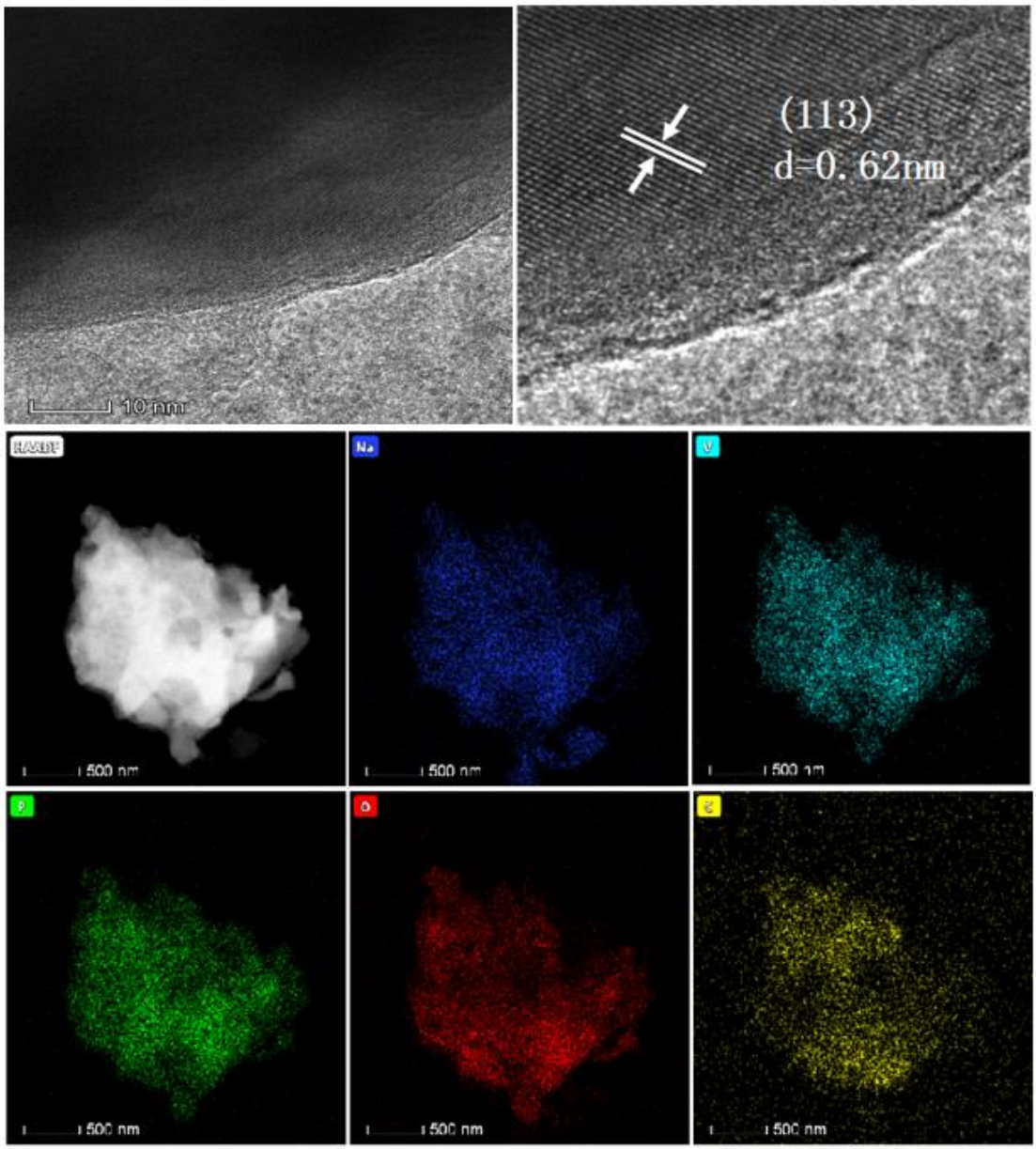

Supplementary Fig. 13 TEM images of NVP&CNTs. The TEM image of shows the cross-linked composite of NVP and CNTs, which can provide effective and intimate contact between NVP and CNTs. The d-spacing of 0.62 nm corresponds to the (113) crystal plane of NVP, suggesting its highly crystalline characteristics. TEM-EDS mapping shows the uniform distribution of Na, V, P, O and C.

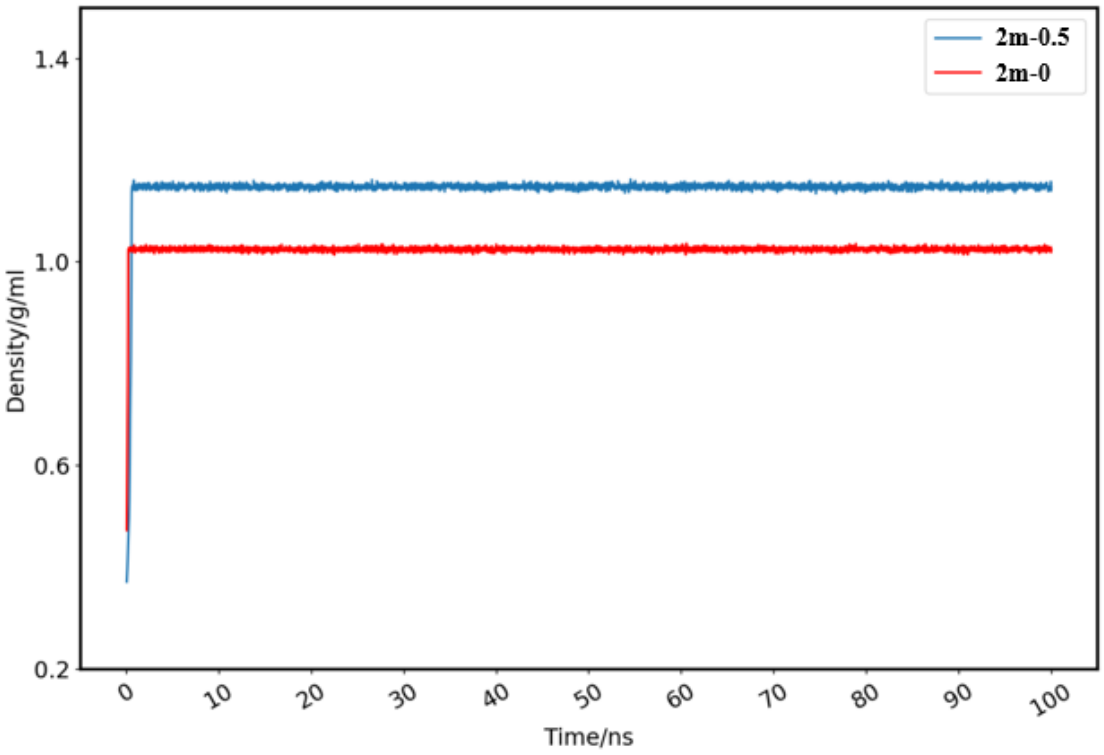

Supplementary Fig.14 System density profile during 100 ns MD simulation.

Supplementary Table 1. Force Field Parameters used in this study

Bonds	K_b(kcal mol^{-1}Å^{-2})	r_0 (Å)		
S-O	570.0	1.53		
C-S	227.0	1.81		
C-H	340.0	1.09		
Cl-O(NaClO4)	216.0	1.76		
HW-HW	553.0	1.51		
OW-HW	553.0	0.96		
Angles	K_θ(kcal mol^{-1} rad^{-2})	θ_0(deg)		
H-C-S	50.0	109.50		
C-S-C	62.0	97.40		
O-S-C	80.0	106.75		
H-C-H	35.0	109.50		
O-Cl-O($NaClO_4$)	70.0	109.47		
HW-OW-HW	100.0	104.52		
HW-HW-OW	0.0	127.74		
Dihedral	IDIVF[a]	K_Φ(kcal mol^{-1} rad^{-2})	Phase(deg)	Periodicity
X-S-C-X	3.0	0.85	0	3

[a] Factor by which the torsional barrier K_Φ is divided

Supplementary Table 2. Details of the simulated models

	2m $NaClO_4$ - 0.5 X_{DMSO}	2m $NaClO_4$ - 0 X_{DMSO}
Number of $NaClO_4$	40	40
Number of DMSO	428	0
Number of Water	482	2181
Equilibrium volume($Å^3$)	66628.34	70044.86
Temperature(K)	300K	300K
Equilibrium density(g/cm^3)	1.15	1.01